Electronic Supplementary Material (ESI) for Nanoscale.

Supplementary Information

Transformative Piezoelectric Enhancement of P(VDF-TrFE) Synergistically Driven by Nanoscale Dimensional Reduction and Thermal Treatment†

G. Ico,[a] A. Myung,[a] B.S. Kim,[b] N.V. Myung[c] and J. Nam*[a]

[a.] Department of Bioengineering
University of California, Riverside
Riverside, CA 92521, USA
E-mail: jnam@engr.ucr.edu

[b.] Korea Institute of Industrial Technology (KITECH)
Incheon 406-840, Korea

[c.] Department of Chemical and Environmental Engineering
University of California, Riverside
Riverside, CA 92521, USA

* Corresponding author. Email: jnam@engr.ucr.edu

Optimization of P(VDF-TrFE) electrospinning conditions

A systematic study of solution tuning including solution conductivity, viscosity, and surface tension was conducted to produce electrospun P(VDF-TrFE) nanofibers with the smallest possible fiber diameter. As a preliminary study, the optimal concentration of salt (pyridinium formate (PF) buffer) to control conductivity of the electrospinning solution was determined; to produce fiber sizes below 100 nm in a DMF/acetone (60/40 vol/vol) solvent system, a maximum of 1.5 wt.% PF, above which electrospraying was exhibited, was determined to increase the conductivity of the solution within an electrospinnable range. Next, to determine optimal factors for viscosity and surface tension, a two-parameter experiment was designed, where the concentration of pyridinium formate (PF) buffer was maintained at 1.5 wt.% in the DMF/acetone solvent system while varying the P(VDF-TrFE) and surfactant (BYK-377)[1] concentrations from 1-2 wt.% and 0.0-0.1 wt.%, respectively. The conductivity of the solutions do not significantly change by varying either P(VDF-TrFE) or BYK-377 concentration. The solution flow rate through a 25-gauge needle at 0.5 ml hr^{-1} and collector distance of 20 cm were kept constant for this and all subsequent experiments, and the applied voltage was adjusted from solution to solution (approx., -15 kV for the solutions tested in this experiment), to maintain the most stable Taylor cone. The environmental conditions for this and all subsequent experiments were kept at 23 °C and an absolute humidity of 7.6 g m^{-3}. Characterization of the resulting fiber morphology was conducted by SEM (**Figure S1a-e**). The fiber diameter as a function of both design parameters shows no distinct trend, mainly due to the lack of fiber formation at low concentrations of P(VDF-TrFE) (**Figure S1f**). Bead density exhibits the expected trend of bead reduction at higher concentrations of P(VDF-TrFE) (**Figure S1g**). Taken together, there is a significant decrease in fiber diameter at the midpoint of each design parameter (i.e., 1.5 wt.% P(VDF-TrFE) and 0.05 wt.% BYK), as well as a significant bead reduction at the same point with an average fiber diameter of 45 nm and bead density of 43,000 beads per mm^2.

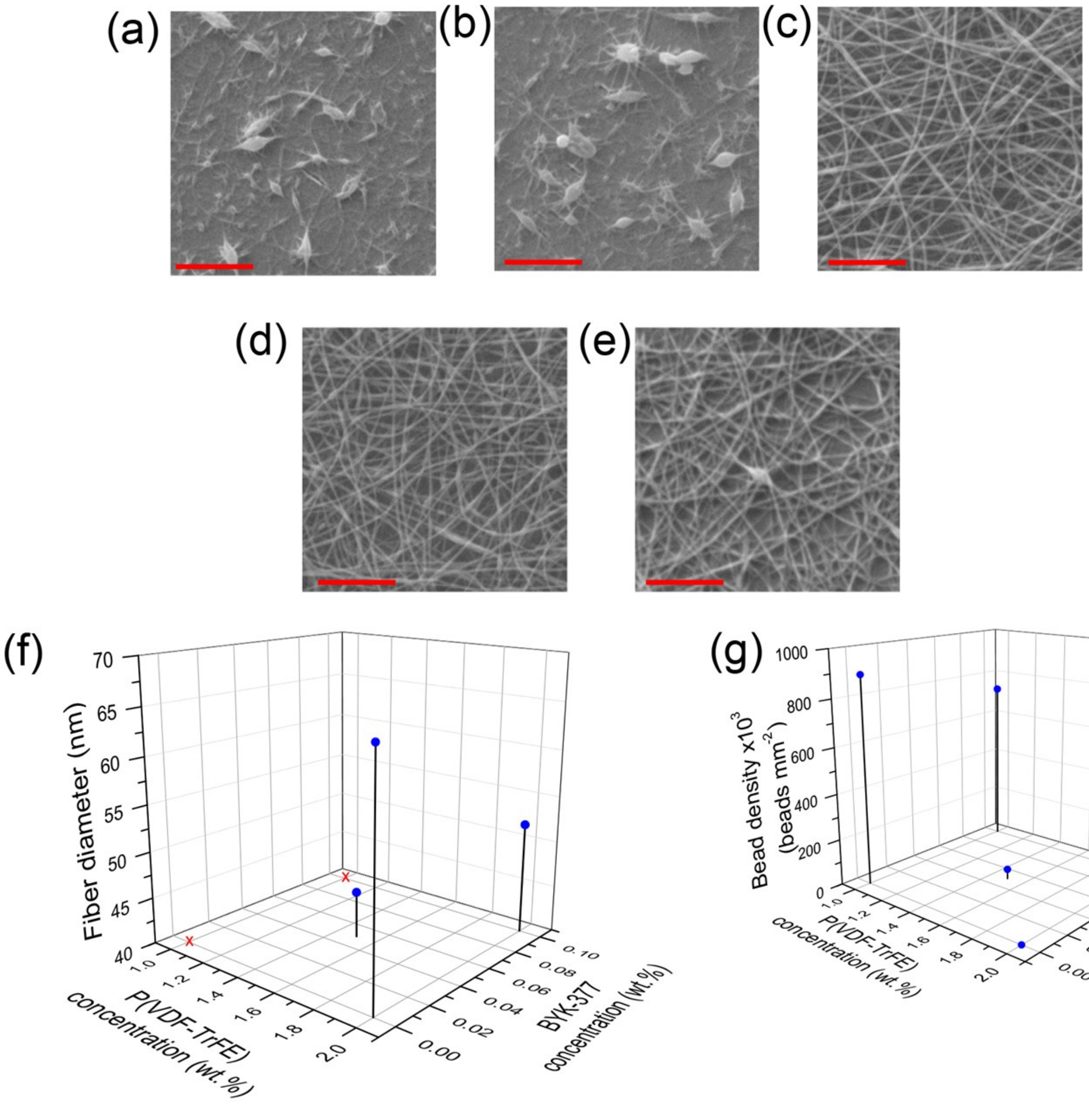

Figure S1. (a-e) Fiber morphologies of corresponding solution from design parameters ((a) 1 wt.% P(VDF-TrFE)/0 wt.% BYK-377, (b) 1/0.1, (c) 2/0, (d) 2/1, and (e) 1.5/0.05 (scale bar = 2 μm)). Quantification of (f) fiber diameter and (g) bead density as a function of design parameters.

Subsequently, a new experiment to tune the proper concentration of P(VDF-TrFE) was conducted with concentrations of 1.5, 1.4, 1.2, 1.1 and 1.0 wt.% with 1.5 wt.% PF in the DMF/acetone solvent system, while maintaining the BYK-377 concentration at 0.05 wt.% determined from the previous experiment. The resulting fiber morphologies are shown in **Figure S2a-f** with arrows in **Figure S2d-f** indicating the presence of a thin film morphology due to unstable electrospinning and solution droplet deposition. **Figure S2g-j** show the fiber diameter distribution and average diameter of each solution except for 1.1 and 1.0 wt.% P(VDF-TrFE) for which thin film formation was observed. **Figure S2k** shows the effect of P(VDF-TrFE) concentration on bead density. From these results, 1.3 wt.%, which resulted in 28 nm average diameter fibers with a bead density of 62,300 beads per mm^2 and slight signs of film morphology, was utilized for further optimization in the next experiments.

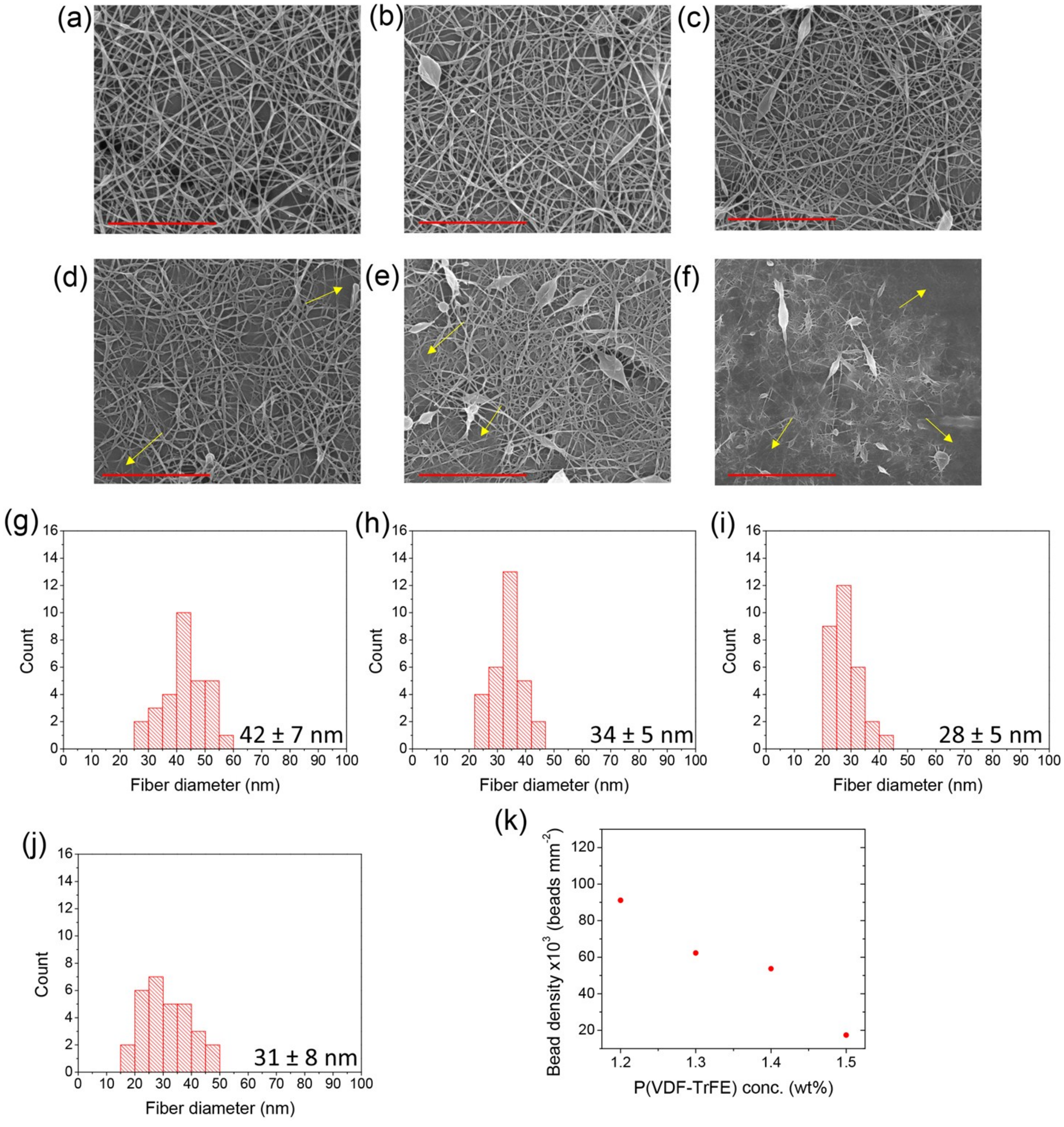

Figure S2. Electrospun P(VDF-TrFE) with various solution concentration between 1.5 and 1.0 wt.% to optimize the synthesis of the smallest fibers without defects. SEM images of (a) 1.5, (b) 1.4, (c) 1.3, (d) 1.2, (e) 1.1, and (f) 1.0 wt.% P(VDF-TrFE) (scale bar = 3 μm). Corresponding fiber diameter distribution of

(g) 1.5, (h) 1.4, (i) 1.3, and (j) 1.2 wt.% P(VDF-TrFE) and bead density as a function of P(VDF-TrFE) concentration (k).

Although it has been shown that utilizing solvents with dielectric constants (ε) of >19 prevents the formation of beads on nanofibers >500 nm, such solutions using solvents with high dielectric values require greater applied voltages to achieve a stable Taylor Cone.[2] The initial solvent system used in this study, composed of DMF (ε=36.7) and acetone (ε=20.7), requires a high and narrow voltage range to maintain a stable Taylor Cone due to the high dielectric constants. The presence of film morphology (**Figure S2c**) likely indicates that the solution requires fine adjustments to prevent solution droplet deposition. Tetrahydrofuran (THF) is a partial solvent of PVDF polymers that has a low dielectric constant (ε=7.6) which can potentially stabilize the electrospinning process. **Figure S3a** shows the fiber morphology from an electrospun solution of 1.3 wt.% P(VDF-TrFE), 1.5 wt.% PF and 0.05 wt.% BYK-377 in THF, replacing DMF/acetone. The fiber size distribution in **Figure S3b** shows that the solution properties still allow for the formation of small fibers even with the low dielectric constant of THF. In spite of no film formation, we observe slight bead formation as well as large agglomerates of polymer, likely due to the partial solubility of P(VDF-TrFE) in THF.

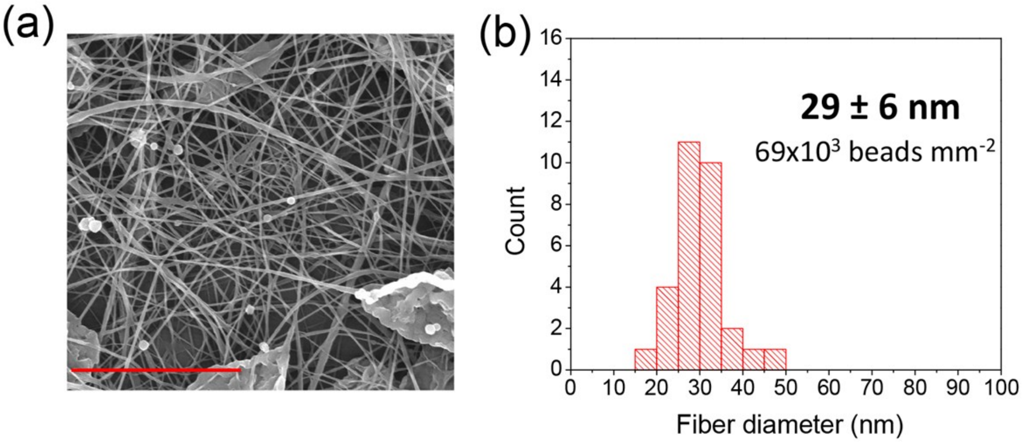

Figure S3 Electrospun P(VDF-TrFE) dissolved in THF. Fiber morphology of electrospun solutions of 1.3 wt.% P(VDF-TrFE) with 1.5 wt.% PF and 0.05 wt.% BYK-377 in (a) THF (scale bar = 3μm) and (b) the resulting fiber distribution.

To increase P(VDF-TrFE) solubility in a THF based solution, we investigated an additive solvent to promote complete dissolution of P(VDF-TrFE) while synthesizing defect-free nanofibers. The use of a Teas solubility graph (**Figure S4a**)[3] predicts that utilizing a DMF/THF mixed solvent system drives the solubility of P(VDF-TrFE) closer to the fractional solubility parameters associated with PVDF (assumed to be similar for P(VDF-TrFE). An electrospinning solution in pure DMF with a close match to the solubility parameters of P(VDF-TrFE) resulted in particle deposition likely due to the unstable electrospinning (**Figure S4b**). By testing various ratios of DMF/THF, we found that an electrospinning solution of 1.3 wt.% P(VDF-TrFE), 1.5 wt.% PF, 0.05 wt.% BYK-377 in a 50/50 (vol/vol) DMF/THF solvent system produced nanofibers with diameters of 32 ± 5 nm (**Figure S4c**), within error of the same solution utilizing pure THF (29 ± 6 nm) (**Figure S4d**), without defects. The resulting viscosity, electrical conductivity, and surface tension of the solution were 2.7 cP, 30.9 μS cm^{-1}, and 22.6 dynes cm^{-1}, respectively. From these systematically designed experiments, we achieved the conditions to produce defect-free P(VDF-TrFE) nanofibers in the range of 30 nm diameter.

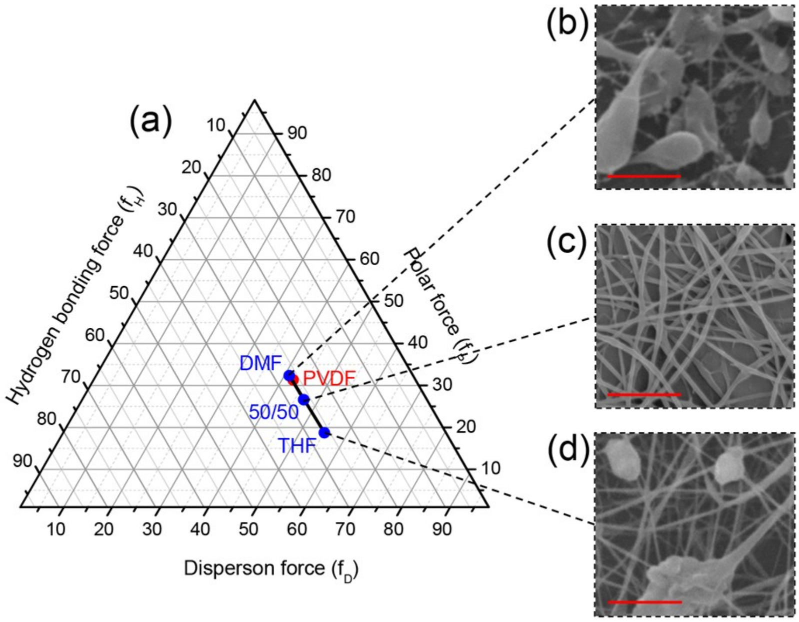

Figure S4. (a) Teas graph showing the relative positions of the fractional solubility parameters of DMF and THF to the parameters of PVDF polymer with the connecting line indicating the path of the solvent mixture ratios. Nanofibers electrospun from 1.3 wt.% P(VDF-TrFE), 1.5 wt.% PF, and 0.05 wt.% BYK-377 in (b) 100% DMF, (c) 50/50 (vol/vol) DMF/THF, and (d) 100% THF solution (Scale bar = 1 μm).

To determine any effects arising from utilizing different solvents to synthesize P(VDF-TrFE) nanofibers, we characterized the piezoelectric response of nanofibers with an approximately 90 nm fiber diameter, synthesized using the DMF/acetone or the DMF/THF solvent system. **Figure S5** shows that the amplitude versus applied voltage response are similar for both conditions, exhibiting similar values of d_{33} for the acetone-based system and THF-based system at $d_{33} = -48.6 \pm 2.8$ pm V^{-1} and $d_{33} = 46.8 \pm 2.0$ pm V^{-1}, respectively.

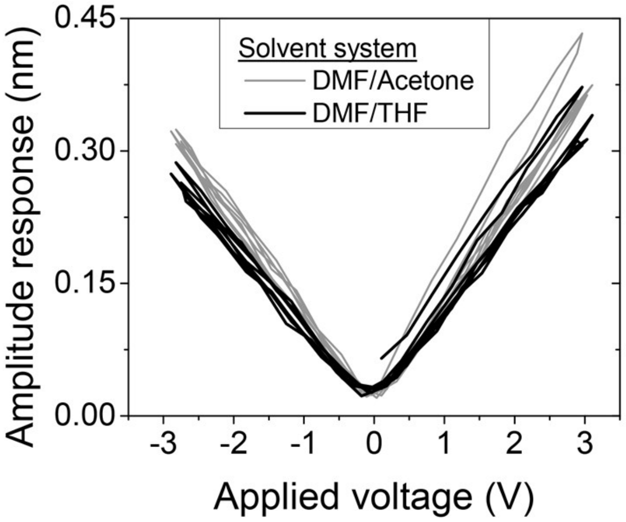

Figure S5. Piezoelectric responses from individual P(VDF-TrFE) nanofibers with a diameter of approximately 90 nm, synthesized by acetone-based or THF-based system.

Table S1. Lattice constants of 30 and 90 nm average diameter P(VDF-TrFE) nanofibers with various thermal treatments.

Sample	Lattice Constants		
	a	b	c
30 nm, 23 °C	8.88	5.12	2.55
30 nm, 90 °C	8.87	5.11	2.55
30 nm, 135 °C	8.92	5.12	2.54
90 nm, 23 °C	8.89	5.17	2.55
90 nm, 90 °C	8.83	5.16	2.52

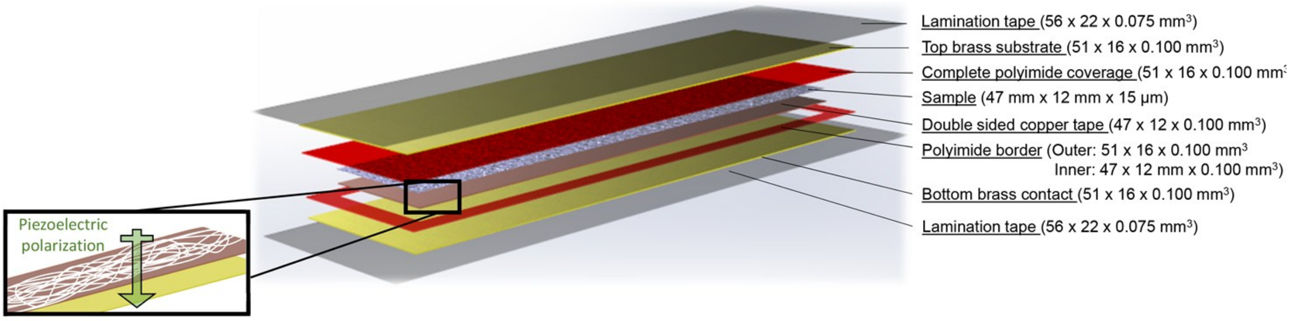

Figure S6. A schematic of the cantilever assembly for the measurements of electric outputs from electrospun P(VDF-TrFE) nanofiber mats. The setup was modified from our previous study.[4] A brass substrate (51 x 16 x 0.100 mm^3) was used as the bottom electrical contact as an exposed area of the brass measured 47 x 12 mm^2, whereas polyimide tape was used to seal the rest of the exposed brass substrate around the working area (51 x 16 x 0.100 mm^3). To promote proper fiber adhesion to the bending substrate, a rectangular strip of double sided adhesive copper foil tape with the same dimensions as the electrode area of the brass was used. The fiber mat sample (47 x 12 x 0.015 mm^3) was placed on top of the adhesive copper. The direction of piezoelectric polarization in the fiber mat is indicated in the inset. A separate brass piece was completely insulated with polyimide tape and placed on top of the bottom assembly to act as the top contact electrode working in capacitive mode. Thin lamination tape was used to seal the structure in a conformal manner and soldered leads were placed on the top and bottom brass pieces to create the final cantilever assembly.

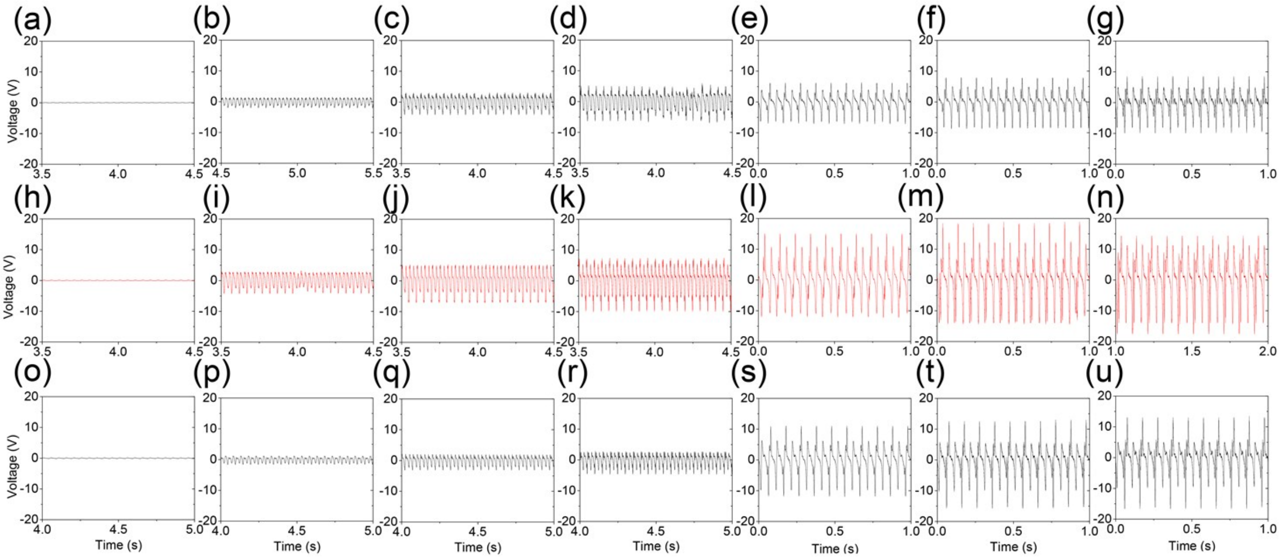

Figure S7. Voltage production of nanofiber mat samples. Raw voltage output of 30 nm average fiber diameter mats which were (a-g) thermal-treated at 23 °C, (h-n) 90 °C, and (o-u) 90 nm average fiber diameter mats at 23 °C. These selected plots represent applied strains of (a,h,o) 0.02%, (b,i,p) 0.05%, (c,j,q) 0.09%, (d,k,r) 0.14%, (e,l,s) 0.19%, (f,m,t) 0.22%, and (g,n,u) 0.26%.

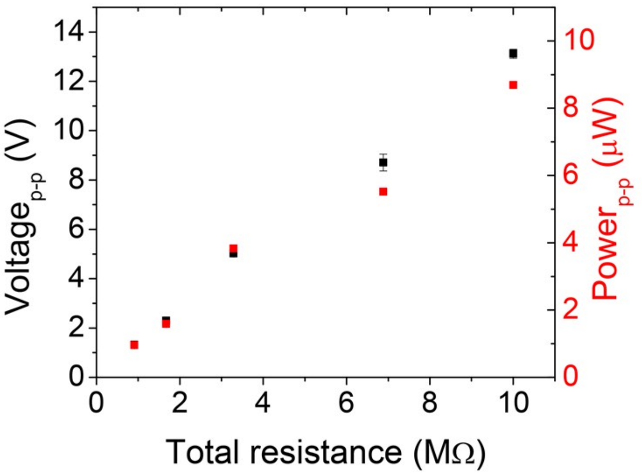

Figure S8. Peak-to-peak voltage and power across varying total resistances. The greatest output voltage and power observed at an open circuit (10 MΩ internal resistance) under a moderate applied strain of 0.14%.

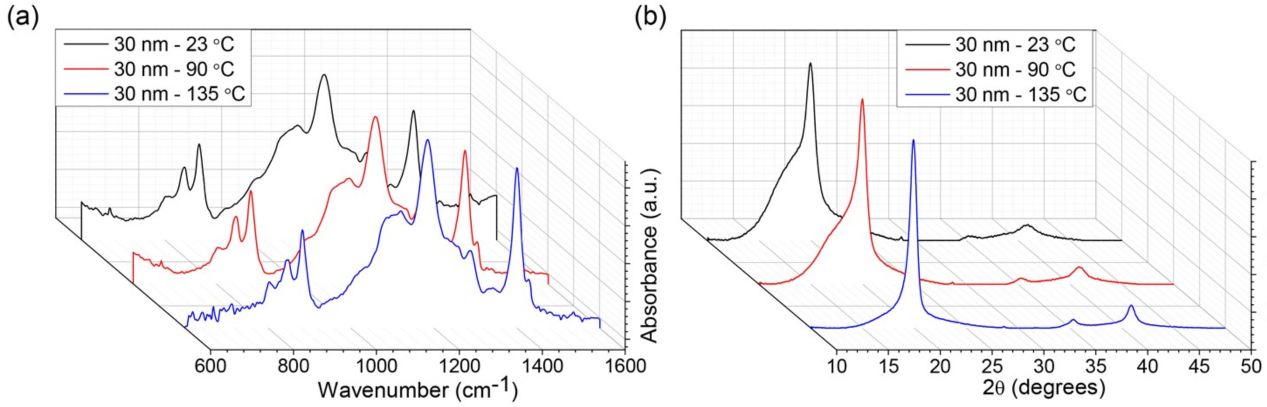

Figure S9. (a) FTIR and (b) XRD spectra of electrospun P(VDF-TrFE) mats composed of nanofibers with an average diameter of 30 nm after various heat treatments. The data were used to quantify electroactive phase content and degree of crystallinity.

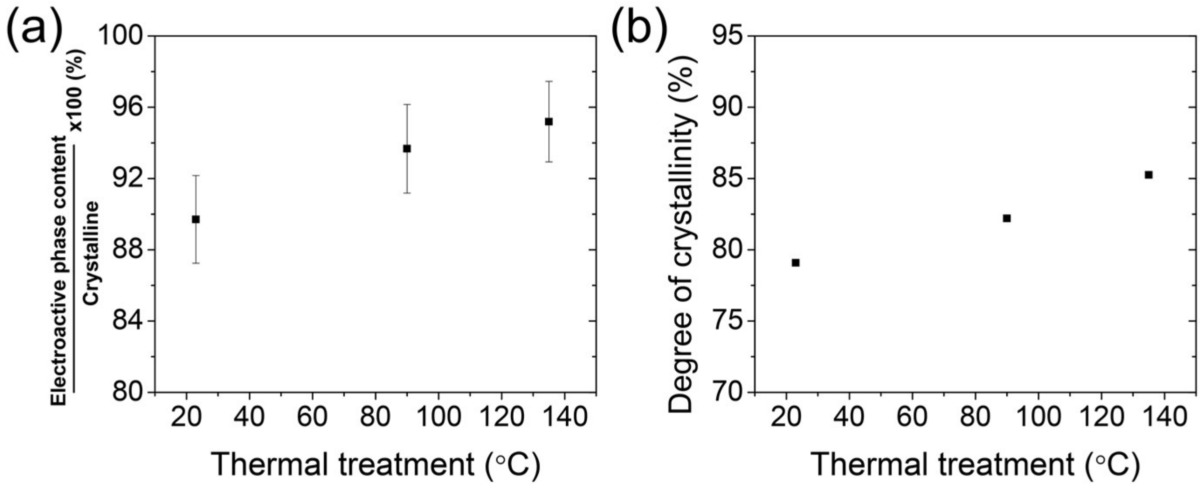

Figure S10. (a) Electroactive phase content and (b) degree of crystallinity of electrospun P(VDF-TrFE) mats composed of nanofibers with an average diameter of 30 nm as a function of temperature.

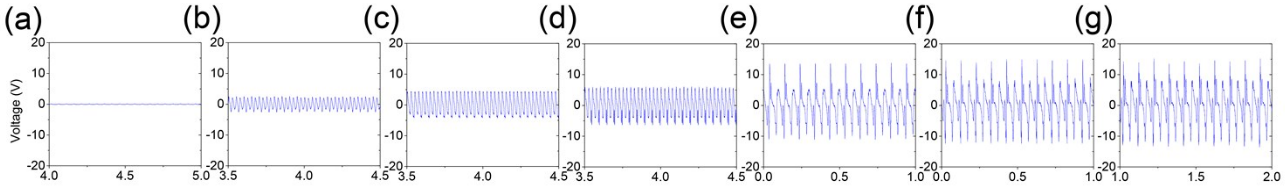

Figure S11. Voltage production of 30 nm average fiber diameter mat samples thermal treated at 135 C. These selected plots represent applied strains of (a) 0.02%, (b) 0.05%, (c) 0.09%, (d) 0.14%, (e) 0.19%, (f) 0.22%, and (g) 0.26%

References

1. M. J. Nalbandian, M. Zhang, J. Sanchez, Y.-H. Choa, D. M. Cwiertny and N. V. Myung, *Journal of Molecular Catalysis A: Chemical*, 2015, 404, 18-26.
2. C. J. Luo, E. Stride and M. Edirisinghe, *Macromolecules*, 2012, 45, 4669-4680.
3. C. M. Hansen, *Hansen solubility parameters: a user's handbook*, CRC press, 2007.
4. G. Ico, A. Showalter, W. Bosze, S. C. Gott, B. S. Kim, M. P. Rao, N. V. Myung and J. Nam, *Journal of Materials Chemistry A*, 2016, 4, 2293-2304.